JOURNAL OF MATERIALS SCIENCE **39** (2004) 6291–6297

Effects of thermal annealing of thin Au film on $Fe_{40}Ni_{38}Mo_4B_{18}$ in ultrahigh vacuum (UHV)

S. K. SHARMA*, V. ZAPOROJTCHENKO, J. ZEKONYTE, A. BUETTNER
Chair for Multicomponent Materials, Faculty of Engineering of Christian-Albrechts University, Kaiserstrasse 2, 24143 Kiel, Germany

S. DEKI
Department of Chemical Science and Engineering, Faculty of Engineering Kobe University, Rokko-dai, Nada, Kobe 657, Japan

F. FAUPEL†
Chair for Multicomponent Materials, Faculty of Engineering of Christian-Albrechts University, Kaiserstrasse 2, 24143 Kiel, Germany
E-mail: ff@tf.uni-kiel.de

Thin films (~20 nm) of Au were vapour-deposited on melt-spun amorphous ribbon specimens of the alloy $Fe_{40}Ni_{38}Mo_4B_{18}$ at room temperature. The specimens were subsequently annealed in UHV (~10^{-8} mbar) at 723 and 823 K in order to observe any dispersion of Au as nanoparticles in the alloy matrix. The motivation for these investigations was derived from similar experiments carried out earlier in nitrogen and in low vacuum conditions, wherein a model based on segregation and oxidation of matrix elements was proposed in order to explain the observed dispersion of Au in the alloy matrix. The present investigations in UHV were carried out as a critical test of this model. However, XPS investigations carried out on these specimens in UHV did not show any dispersion of Au particles after annealing at these temperatures. Further examination of annealed specimen surfaces by SEM and AFM revealed the formation of Au-rich islands on the surface. Native oxide film underneath the Au film and crystallization of the alloy during thermal annealing do not seem to have any effect on depth profiles of Au. These results, when compared with those obtained after annealing the specimens in nitrogen and in low vacuum conditions (~10^{-1}–10^{-3} mbar), are suggestive of the crucial role of the annealing atmosphere during thermal annealing.

1. Introduction

Thermal annealing of a substrate material with a thin metallic film in ultra high vacuum (UHV) or an inert medium is employed to investigate interdiffusion [1]. This route has also been used to prepare metal/polymer composite thin films, in which the metal particles are uniformly dispersed as nano-sized particles within the polymer matrix [2–4]. The technique relies on vacuum vapor deposition of a thin metallic film on an amorphous polymer matrix and its subsequent heat treatment in air or nitrogen atmosphere at temperatures above the crystallization temperature (T_g) of the polymer matrix. This technique, also known as Relaxative Auto-Dispersion (RAD), results in auto-dispersion of nano-sized metallic particles by thermal relaxation and crystallization of the amorphous polymer matrix. It was suggested that crystallization of the amorphous polymer matrix during thermal annealing plays an important role in the dispersion process by imparting additional mobility to metal particles for further penetration into the matrix [3].

The RAD method has recently been employed to obtain dispersion of nano-sized Au particles in a metallic amorphous alloy, namely $Fe_{40}Ni_{38}Mo_4B_{18}$ [5, 6]. Thermal annealing was performed above the crystallization temperature ($T_x = 820$ K at 20 K min^{-1}) in nitrogen atmosphere. It was observed that nano-sized particles of Au dispersed fairly deeply (up to few hundred nanometres) in the metallic matrix. It was also observed that the penetration of Au was limited to much smaller depths if pre-crystallized specimens were employed thus suggesting that the crystallization of the amorphous $Fe_{40}Ni_{38}Mo_4B_{18}$ during heat-treatment played a significant role during the dispersion process like that observed in polymers [3, 4]. Based on these investigations it was suggested that the RAD technique may apply to any amorphous matrix for obtaining the dispersion of nano-sized metal particles [5]. In order to

Present address: Department of Physics, Malaviya National Institute of Technology, Jaipur 302 017, India.
†Author to whom all correspondence should be addressed.

gain a detailed understanding of this dispersion process in metallic amorphous alloys we carried out further investigations using specimens with thin Au film on amorphous $Fe_{40}Ni_{38}Mo_4B_{18}$. The results of our investigations on annealing effects of thin Au film on $Fe_{40}Ni_{38}Mo_4B_{18}$ in nitrogen and in low vacuum conditions ($\sim 10^{-1}$–10^{-3} mbar) did, indeed, show depth distribution of Au up to several hundred nanometers in the alloy, but no significant effect of crystallization on transport of Au atoms during thermal annealing was observed [7]. It was suggested that the driving force for Au dispersion in the alloy is provided by the surface segregation and the reactivity of the matrix elements with residual oxygen present in the annealing medium [7].

In order to test the crucial influence of the annealing medium and the ideas proposed in the above model for the observed dispersion of Au [7], the motivation for the present investigation was derived from the following: (i) if the annealing environment (i.e., nitrogen or low vacuum $\sim 10^{-1}$–10^{-3} mbar) is not important for the process, then it should be possible to observe this dispersion of nano-sized Au particles by thermal annealing of a thin Au film on $Fe_{40}Ni_{38}Mo_4B_{18}$ (henceforth referred in the text as Au/$Fe_{40}Ni_{38}Mo_4B_{18}$) under clean conditions also, i.e., in ultra-high vacuum, and (ii) no dispersion should be observed during heat treatment of Au film on pre-crystallized specimens. Therefore, the present study was undertaken with a view to examine the above points. In addition, the role of the native oxide film on the alloy underneath the Au film during thermal annealing of Au/$Fe_{40}Ni_{38}Mo_4B_{18}$ is also investigated. The results of thermal annealing of Au/$Fe_{40}Ni_{38}Mo_4B_{18}$ carried out in UHV are presented in this study.

2. Experimental

Specimens (10 mm $\times$ 10 mm) were cut from an amorphous melt-spun ribbon (25 μm thick) of $Fe_{40}Ni_{38}Mo_4B_{18}$ (from Allied Chemicals sold under the trade name Metglass 2826 MB). The specimens were cleaned ultrasonically in iso-propanol and dried under a jet of pressurized air and were mounted on the substrate holder of the high vacuum vapor deposition unit. A thin ($\sim$20 nm thickness) film of Au was vapor deposited on these specimens using a vacuum vapor deposition system under a vacuum of $\sim 1 \times 10^{-6}$ mbar. The deposition was controlled by using a quartz crystal microbalance and the typical deposition rate was maintained at about 0.5 nm min^{-1}.

The heat-treatments of Au-deposited amorphous $Fe_{40}Ni_{38}Mo_4B_{18}$ specimens were carried out at 723 and 823 K in UHV conditions ($\sim 10^{-8}$ mbar) in a preparation chamber attached to the photoelectron spectrometer. The alloy showed two exothermic crystallization peaks at 722 and 820 K in a DSC scan recorded at a heating rate of 20 K min^{-1}. The specimens with Au film on pre-crystallized and sputter-cleaned $Fe_{40}Ni_{38}Mo_4B_{18}$ were prepared *in-situ* inside the preparation chamber. The pre-crystallized specimens were obtained by subjecting the amorphous specimens to a heat-treatment at 823 K for 120 min in UHV. The specimens were sputter cleaned with 5 keV Ar^+ ions in order to remove the native oxide film before depositing $\sim$ 20 nm thick Au film using the Au evaporator inside the preparation chamber. The removal of the native oxide film was checked by measuring the O 1s XPS peak intensity which was reduced to a minimum background level after sputter cleaning of the specimen. It was, however, not possible to completely get rid of these impurities and the observation of very small signals of oxygen and carbon even after prolonged sputtering may perhaps indicate their presence in the alloy in dissolved form in trace amounts (cf. Fig. 3 given later).

The depth profiles of Au from as-deposited and annealed specimens were obtained by recording XPS peaks of the alloy constituents using an Electron Spectrometer (Model Omicron Fullab) in conjunction with argon ion sputtering. The sputtering was performed using Ar^+ ions of 5 keV energy at a typical beam current of about 70 nA under argon gas pressure of about 6×10^{-6} mbar. At this ion beam energy and current a sputter rate of about 0.25 nm min^{-1} was gravimetrically estimated. The spectrometer was equipped with a electrostatic hemispherical analyzer and a dual anode source with a possibility to use either Al K_α (energy = 1486.6 eV) or Mg K_α (energy = 1253.6 eV) X-rays. The XPS peaks of Au 4f, Fe 2p, Ni 2p, O 1s, C 1s and other alloy constituents were recorded using Mg K_α X-rays at an analyzer pass energy of 100 eV. The XPS O 1s peak was recorded using Al K_α X-rays as the O1s peak interferes with Auger peak (LMM) of Fe when recorded using Mg K_α X-rays. Surface morphologies of some of the specimens were examined by scanning electron microscopy (SEM) using a Philips SEM (Model No. Philips XL 30) which also had an attached EDAX (spatial resolution 1μm) unit for carrying out energy dispersive X-ray analysis from regions of interest in the SEM micrograph.

3. Results and discussion

Fig. 1 depicts the plot of the intensity of Au 4f peak from the as-deposited and annealed specimens (annealed at 823 K for 120 min) as a function of sputtering depth. The intensity ratio was normalized by its value on the as-received surface of the specimen in each case, i.e., the value before sputtering the specimen with Ar^+ ions. The following observations are made from this figure:

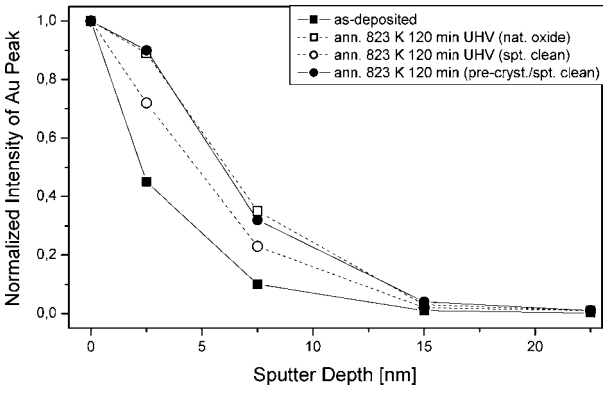

Figure 1 Depth profiles of Au after heating of Au/$Fe_{40}Ni_{38}Mo_4B_{18}$ at 823 K for 120 min in UHV.

(i) there is no long range diffusion or dispersion of Au after annealing the specimens at 823 K for 120 min in UHV as seen from the depth profiles for annealed specimens. A slight profile broadening as seen in profiles from annealed specimens may as well arise from the surface roughness introduced after annealing [8]; (ii) depth profiles from the specimens with native oxide underneath the Au-film and that from the Au-film on the sputter cleaned (without native oxide) specimen are practically similar thus suggesting that the native oxide layer seems to play no significant role during the heat treatment, i.e., it does not lead to any significant changes in the depth profiles of Au, (iii) depth profile from the pre-crystallized specimen is also similar to those observed from amorphous specimens and this observation clearly shows that the crystallization during heat treatment at 823 K for 120 min in UHV does also have no influence on the depth profile of Au. It can thus be concluded from these observations that the thermal annealing of thin Au film on $Fe_{40}Ni_{38}Mo_4B_{18}$ at 823 K in UHV does not result in any long range diffusion or dispersion of Au in the alloy matrix. This observation is in sharp contrast to the long-range dispersion of Au observed in the same alloy after annealing in nitrogen atmosphere and in low vacuum conditions ($\sim 10^{-1}$–10^{-3} mbar) at the same temperature [5–7]. It is thus suggested that the annealing environment, i.e., nitrogen or low vacuum ($\sim 10^{-1}$–10^{-3} mbar) may perhaps be crucial for obtaining dispersion of Au particles in this alloy.

Fig. 2 shows the plot of the (Au/Fe) intensity ratio derived from the peak areas of the XPS peaks of Au 4f and Fe 2p as a function of annealing time for the specimen annealed at 823 K in UHV. The Au film was deposited on this specimen after cleaning it in iso-propanol ultrasonically and no sputter cleaning was done to remove the native oxide before Au deposition. It is interesting to note from this figure that a sharp decrease in the (Au/Fe) intensity ratio is observed after 30 min of annealing and further annealing for longer times shows only little changes in the intensity ratio. These observations point to the following: the Au-film is no longer continuous after thermal annealing and perhaps has transformed into

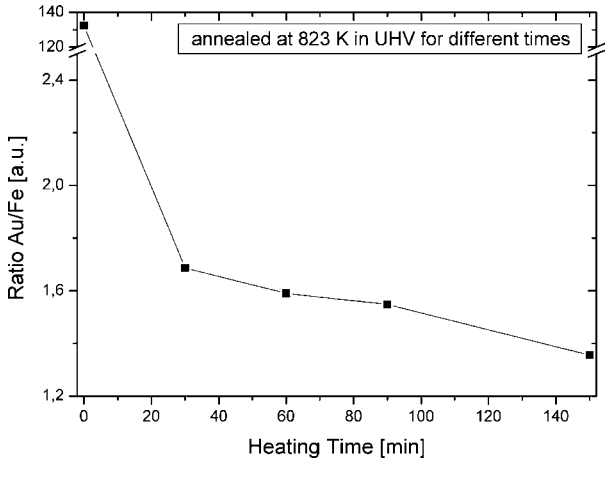

Figure 2 XPS intensity ratio (Au/Fe) derived from peak area of Au 4f and Fe 2p XPS peaks as a function of annealing time after heating a $Au/Fe_{40}Ni_{38}Mo_4B_{18}$ specimen at 823 K in UHV.

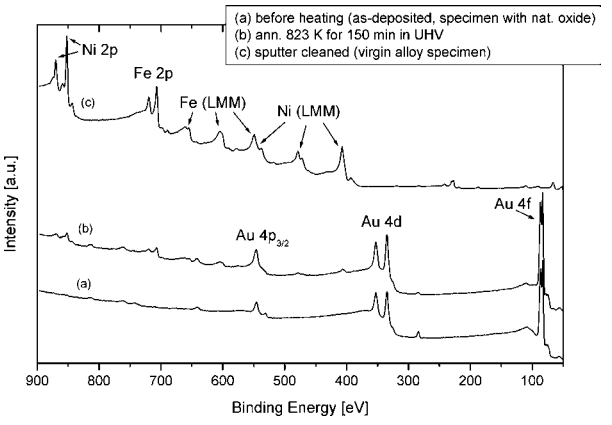

Figure 3 XPS survey spectra recorded from: (a) as-deposited specimen, (b) after heating at 823 K for 150 min in UHV and (c) virgin sputter cleaned specimen.

Au islands/clusters and hence a sharp decrease in Au intensity and a rise in Fe intensity from the matrix could be explained. The second possibility could be that Fe segregated to the Au surface through the grain boundaries of Au-film during annealing. In this context it is worth mentioning here that intensity of Ni also followed the same trend as that of Fe, but no peaks due to other matrix elements, i.e., Mo and B could be detected on the surface after annealing (cf. Fig. 3 given later). Before commenting further on these possibilities, it would be interesting to look at some more observations in the following.

Fig. 3 shows the XPS survey spectra from a Au-deposited specimen (with native oxide) before and after heating at 823 K in UHV along with a spectrum after prolonged sputtering of a virgin specimen. The spectrum before heating (Fig. 3a) shows Au peaks as major peaks in addition to small peaks due to C and O, while in the spectrum after heating at 823 K for 150 min (Fig. 3b) additional clear peaks due to Fe and Ni can also be seen. Interestingly, no peaks due to B and Mo (which are also matrix constituents) are visible in the spectrum after heating (Fig. 3b), which, however, can be clearly seen in the spectrum recorded from a sputter cleaned specimen (Fig. 3c). The role of temperature in controlling the segregation of the matrix elements Fe (or Ni) is obvious from the next figure (Fig. 4) which depicts a typical plot of the normalized peak intensity for Fe 2p XPS peak (I_{Fe}) (normalized by sum of the peak intensities of Fe 2p (I_{Fe}) and Au 4f (I_{Au}), i.e., the intensity ratio $I_{Fe}/(I_{Fe} + I_{Au})$, from specimens annealed at 723 and 823 K for the same annealing time (300 min). It is seen from this figure that no Fe is found on the surface after annealing at 723 K in contrast to that shown by the specimen annealed at 823 K and an increased amount of Fe is seen on the specimen annealed at higher temperature. It is worth mentioning here that in addition to temperature (Fig. 4) and time (cf. Fig. 2) in governing the kinetics of the process during annealing, the other important controlling factors include annealing environment and film thickness. The effect of Au film thickness during annealing has, however, not been investigated.

The individual peaks for Au 4f, Fe 2p and Ni 2p are shown in Fig. 5a–c and the peaks due to Au $4f_{7/2}$, Fe

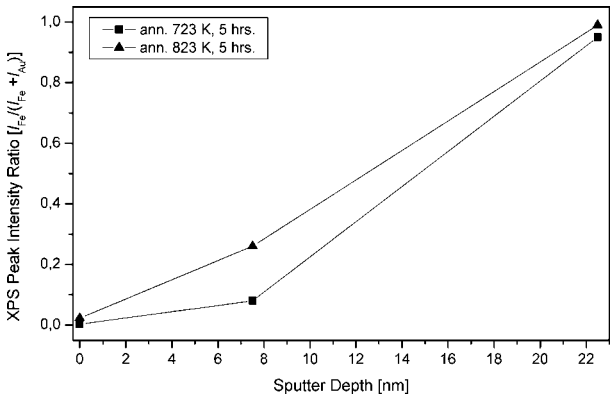

Figure 4 A typical plot of the intensity of the Fe 2p XPS peak (I_{Fe}) normalized by sum of the intensities of Fe 2p (I_{Fe}) and Au 4f (I_{Au}) XPS peaks, i.e., the XPS peak intensity ratio $I_{Fe}/(I_{Fe}+I_{Au})$, as a function of depth for two specimens annealed at 723 and 823 K for the same time, i.e., 300 min.

$2p_{3/2}$ and Ni $2p_{3/2}$ appeared at 83.8 eV, 707.6 eV and 852 eV, respectively. There is no change in the peak position or shape of the Au peak (Fig. 5a), but a clear broadening and a hump towards high binding energy side in the peaks of Fe 2p and Ni 2p (Fig. 5b and c) after heating is quite noteworthy. It suggests that after heating Fe and Ni partly get transformed into oxide form [7, 9], picking up oxygen most likely from the residual oxygen in the chamber. The other possible sources of O could be the oxygen in the native oxide film between Au film and the alloy and the oxygen present as impurity in trace amount in the alloy matrix in dissolved form (cf. Fig. 3c). In order to check this point O 1s peak was also recorded after heating which appeared at 533 eV (Fig. 5d). The Fig. 5d also shows the O 1s peak appearing at 531.3 eV recorded from a virgin alloy specimen after a prolonged sputter cleaning with 5 keV Ar^+ ions. Therefore, the peak position of O 1s peak at 533 eV and the observed humps at high binding energy side in Fe 2p and Ni 2p spectra are suggestive of a partial oxidation of these elements after heating [7, 9].

The above discussion suggests that the heating of $Au/Fe_{40}Ni_{38}Mo_4B_{18}$ at 823 K for 150 min in UHV results in a drastic reduction in the intensity ratio of (Au/Fe) and in the appearance of additional peaks due to the matrix elements Fe and Ni which exist partly in non-metallic (oxide) form. In order to seek further explanation for these effects the surface morphology of the specimen was examined by SEM. This is shown in the micrograph in Fig. 6 where some island formation on the surface is clearly seen. An EDAX analysis (Fig. 7) of these island regions confirmed them to be Au-rich (Fig. 7a), while the surrounding matrix was depleted in Au and richer in matrix elements Fe and Ni (Fig. 7b). It thus becomes clear from Figs 6 and 7 that heating the specimen in UHV resulted in transformation of Au film into small Au-rich islands on the surface. This observation also explains the conclusions drawn earlier from Figs 1 and 2.

In order to understand the formation of Au-rich islands on the surface after thermal annealing, it is noteworthy that Au has low solubility in both Fe and Ni at these temperatures and there is a large miscibility gap in Au-Ni system [10]. Also the heat of mixing

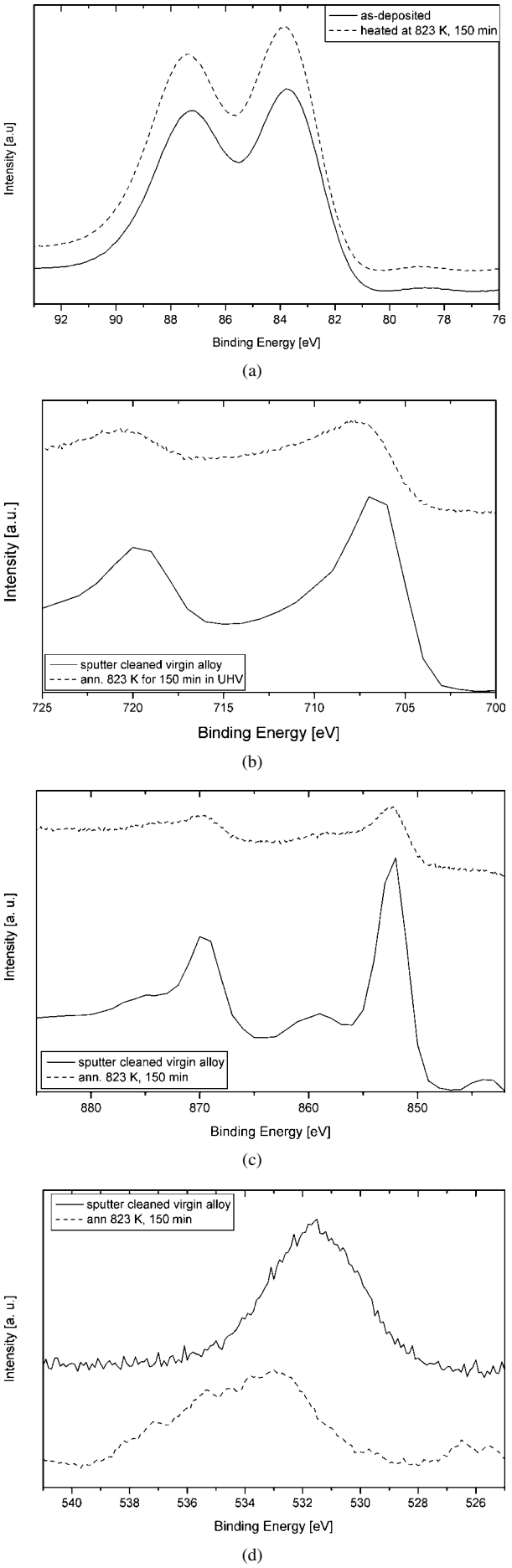

Figure 5 XPS peaks for (a) Au 4f, (b) Fe 2p, (c) Ni 2p, and (d) O 1s after heating $Au/Fe_{40}Ni_{38}Mo_4B_{18}$ specimen at 823 K for 150 min in UHV. Respective peaks from sputter cleaned surface of the virgin alloy are also shown.

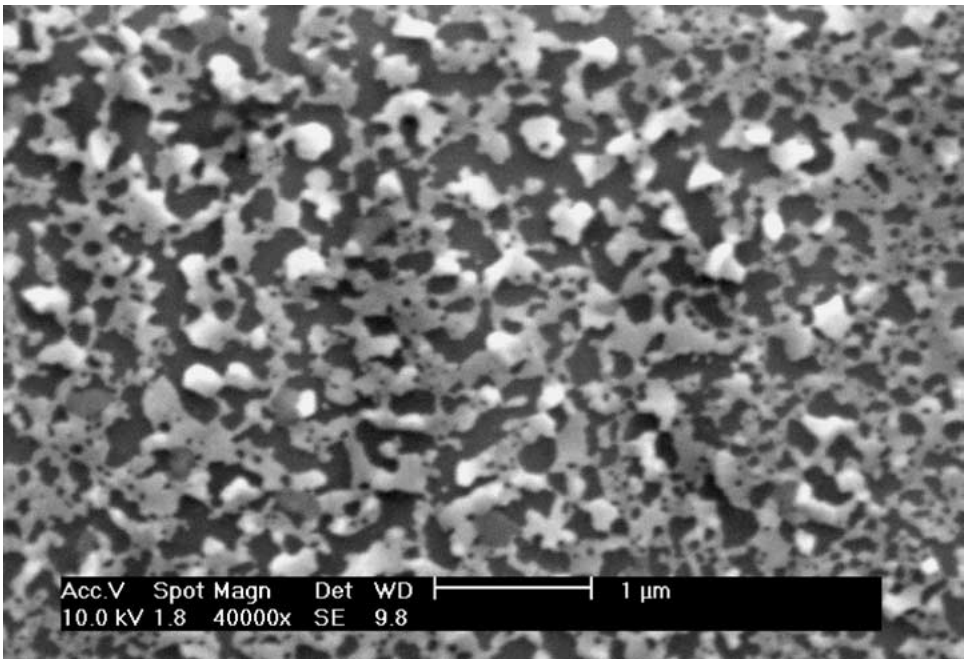

Figure 6 SEM micrograph from a specimen heated at 823 K for 150 min in UHV showing the formation of Au-rich islands (the bright regions) on surface after annealing.

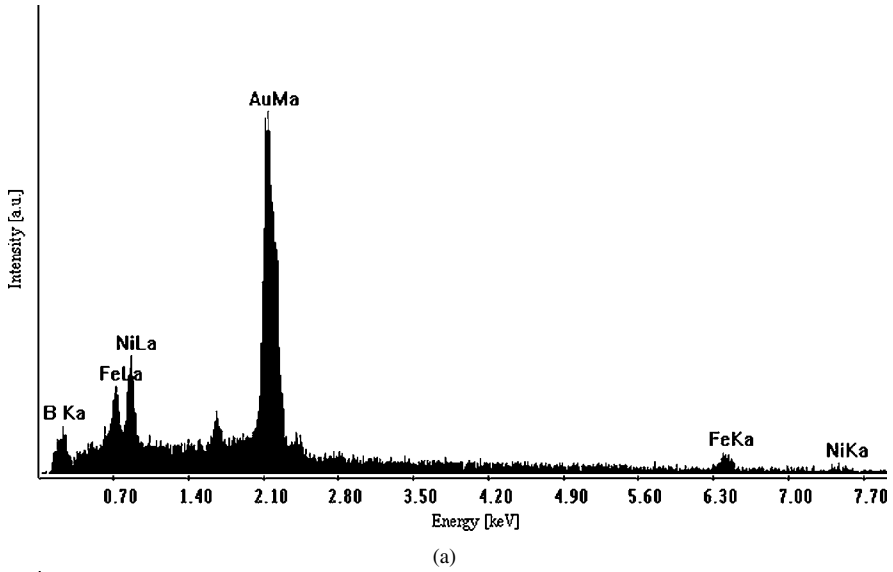

(a)

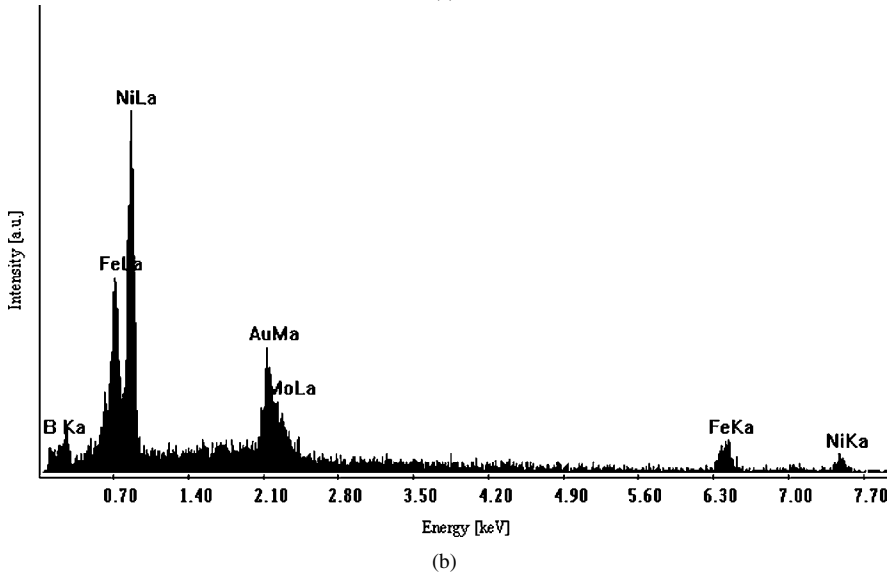

(b)

Figure 7 Typical EDAX spectra from bright and dark regions in Fig. 6. The bright regions represent Au-rich islands (a) while the dark regions represent Fe- and Ni-rich surrounding matrix (b).

for liquid binary alloys of Au with Fe (ΔH_{mix} = +8 kJ mol^{-1}) or Ni (ΔH_{mix} = +7 kJ mol^{-1}) is positive [11] suggesting repulsive interaction of Au with these elements and thus clustering tendencies of Au after heating Au/$Fe_{40}Ni_{38}Mo_4B_{18}$ can be understood [12]. It is thus suggested that as a result of heating Au/$Fe_{40}Ni_{38}Mo_4B_{18}$ at 823 K in UHV, both Fe and Ni diffuse out through grain boundaries of Au film and any presence of oxygen during heating (e.g., residual oxygen in the chamber) provides additional driving force for segregation of these elements to the surface due to their much stronger affinity for oxygen (residual oxygen in the chamber) than that of Au and at the same time some surface alloying between Au-Fe and Au-Ni is not ruled out. However, the absence of segregation of another reactive and small-sized matrix element B is certainly quite noteworthy and needs explanation. It is difficult to pin-point the exact reasons for the absence of B segregation, it is possible that the reaction kinetics is predominantly controlled by the out-diffusion of Fe and Ni and the tendency of Au for clustering which results in the break-up of Au film into small Au-rich islands. Further, it is likely that there is no enough chemical driving force available for segregation of B to the surface during thermal annealing in UHV due to its strong tendency for oxidation and in such a case an oxidation-driven strong segregation of B might occur if annealing was carried out in an environment containing reasonable amount of oxygen required for sustaining this reaction. This, indeed, was observed during thermal annealing of these specimens in nitrogen and in low vacuum conditions ($\sim 10^{-1}$–10^{-3} mbar) and was attributed to the presence of residual oxygen in the annealing media [7]. The amount of residual oxygen in the annealing medium thus has a strong influence in controlling the kinetics of the observed segregation of the matrix elements.

It is interesting to note here that the depth profiles of Au in Fig. 1 are not suggestive of any significant diffusion of Au into the alloy $Fe_{40}Ni_{38}Mo_4B_{18}$. On the other hand, based on the reported Au diffusivity data in some Fe-based amorphous alloys [13, 14] a significant profile broadening due to diffusion would have been expected. In this context, it should be noted that the reported data for Au diffusion in Fe-based amorphous alloys [13, 14] were obtained after diffusion annealing in high vacuum ($\sim 10^{-5}$ mbar) and not in UHV ($\sim 10^{-8}$ mbar) as carried out in the present investigation. This contrasting difference in the diffusion behavior in UHV and in high vacuum again point to the possibility of the crucial effect of annealing medium on diffusion behavior of Au in Fe-based amorphous alloys. In this context, it is further interesting to note that no diffusion of Ag was observed in $Fe_{40}Ni_{38}Mo_4B_{18}$ at these temperatures [15]. These measurements were carried out using a thin silver tracer film on the alloy and its subsequent annealing in ultra high vacuum conditions [15]. These observations are similar to those made in the present study where no significant diffusion of Au was observed after thermal annealing of thin Au film on $Fe_{40}Ni_{38}Mo_4B_{18}$ in UHV. The absence of significant Au diffusion in the alloy $Fe_{40}Ni_{38}Mo_4B_{18}$ after thermal annealing in UHV further supports the view that the reaction kinetics at these temperatures and under our experimental conditions is controlled by the faster diffusing and smaller Fe and Ni matrix atoms than the bigger Au atoms. Therefore, it can be concluded from the above discussion that the low solubilities of Fe and Ni in Au and their positive heat of mixing with repulsive interaction and the tendency of Fe and Ni for surface segregation are major factors that more likely lead to the transformation of initial Au film into small Au-rich islands after thermal annealing in our investigations. Such formation of Au-rich islands in Au-Ni thin films during annealing at similar temperatures has earlier been reported [16–18].

4. Summary

To summarize, our observations on heating of a thin Au film on amorphous $Fe_{40}Ni_{38}Mo_4B_{18}$ in UHV at 823 K revealed the formation of Au-rich islands on the surface, but no long range diffusion or dispersion of Au as nano-particles in the alloy was observed, which is in sharp contrast to the results of some investigations when annealing was done in nitrogen atmosphere and in low vacuum conditions ($\sim 10^{-1}$–10^{-3} mbar) [5–7]. It is thus suggested that the annealing atmosphere (other than UHV) plays a crucial role in dispersion of metal particles during thermal annealing and the results of the present study corroborate our ideas in the proposed mechanism for observed Au dispersion effects after annealing Au/$Fe_{40}Ni_{38}Mo_4B_{18}$ in annealing environments, like nitrogen and low vacuum ($\sim 10^{-1}$–10^{-3} mbar) which contain increased amounts of residual oxygen [7]. More details on the effects of annealing Au/$Fe_{40}Ni_{38}Mo_4B_{18}$ in nitrogen atmosphere and in low vacuum conditions ($\sim 10^{-1}$–10^{-3} mbar) leading to diffusion and dispersion of metal particles in this alloy can be found in [7].

Acknowledgements

We thank Dr. K. Raetzke and Mr. J. Erichsen for critical reading of the manuscript. Thanks are due to Mr. S. Rehders and Mr. Thomas Metzing for their help in furnace set-up for annealing in nitrogen and to Mrs. M. Schwitzke for her help in SEM investigations. One of us (S. K. Sharma) would like to gratefully acknowledge the invitation and the financial support received for working as a Visiting Scientist at the Lehrstuhl für Materialverbunde, Kiel University, Kiel (Germany).

We gratefully acknowledge financial support form Deutsche Forschungsgemeinschaft (DFG) (Grant number Fa234/6-1) and Japanese Society for the Promotion of Science (JSPS).

References

1. J. M. POATE, K. N. TU and J. W. MAYER, "Thin Films: Interdiffusion and Reactions" (Wiley, NY, 1978).
2. T. NOGUCH, K. GOTOH, Y. YAMAGUCH and S. DEKI, *J. Mater. Sci. Lett.* **10** (1991) 648.
3. K. AKAMATSU and S. DEKI, *J. Coll. Interf. Sci.* **214** (1999) 353.
4. S. DEKI, K. SAYO, T. FUJITA, A. YAMADA and S. HAYASHI, *J. Mater. Chem.* **9** (1999) 943.

5. T. YANO, "Solid Phase Dispersion Through Thermal Relaxation Process," Master Thesis, Division of Industrial Chemistry, Graduate School of Engineering, Kobe University Japan, Thesis No. 920T219T, 1999.
6. S. DEKI, "Division of Industrial Chemistry," Graduate School of Engineering, Kobe University, Japan 2001 (private communication).
7. S. K. SHARMA, V. ZAPOROJTCHENKO, J. ZEKONYTE, S. DEKI and F. FAUPEL, *Mater. Sci. Engng.* A **351**(1/2) (2003) 316.
8. Y. WATANABE, Y. NAKAMURA, S. HIRAYAMA and N. TANIGUCHI , *J. Vac. Sci. Technol.* B **13** (1995) 1207.
9. J. F. MOULDER, W. F. STICKLE, P. E. SOBOL and K. D. BOMBEN, "Handbook of X-ray Photoelectron Spectroscopy" (Perkin Elmer Corporation, Physical Electronics Division, Minnesota, USA, 1992).
10. E. A. BRANDES and G. B. BROOK (eds.), "Smithells Metals Reference Book" (Butterworth Heinmann, Oxford, 1998).
11. F. R. DE BOER, R. BOOM, W. C. M. MATTENS, A. R. MIEDEMA and A. K. NIESSEN, "Cohesion in Metals, Transition Metal Alloys" (North Holland, Amsterdam, 1988).
12. Y. ZHANG, U. CZUBAYKO, N. WANDERKA, F. ZHU, and H. WOLLENBERGER, *J. Mater. Res.* **15** (2000) 1271.
13. D. AKHTAR, B. CANTOR and R. W. CAHN, *Acta Metall.* **30** (1982) 1571.
14. S. K. SHARMA, S. BANERJEE, KULDEEP and A. K. JAIN, *ibid.* **36** (1988) 1683.
15. S. LENSER, V. ZOELLMER, J. ERICHSEN, S. DANIEL, K. RAETZKE, S. DEKI and F. FAUPEL, *Scripta Materialia.* **48** (2003) 275.
16. D. QIAO, L. S. YU, S. S. LAU, L. Y. LIN, H. S. JIANG and T. E. HAYNES, *J. Appl. Phys.* **88** (2000) 4196.
17. L. CHEN, F. R. CHEN, J. J. KAI, L. CHANG, J. K. HO, C. S. JONG, C. C. CHIU, C. N. HUANG, C. Y. CHEN and K. K. SHIH, *ibid.* **86** (1999) 3826.
18. J. K. SHEU, Y. K. SU, G. C. CHI, W. C. CHEN, C. Y. CHEN, C. N. HUANG, J. M. HONG, Y. C. YU, W. WANG and E. K. LIN, *ibid.* **83** (1998) 3172.

Received 28 May 2003
and accepted 11 May 2004